Puzzling solid-liquid phase transition of water(mW) from Free Energy Analysis: A Molecular Dynamics Study

Chandan K Das*

Department of Chemical Engineering, National Institute of Technology Rourkela Rourkela, India-769008.

*Corresponding author E-mail:dasck@nitrkl.ac.in,

λ Current address: *National Institute of Technology Rourkela, Rourkela, India-769008.*

Acknowledgements: This work is supported by National Institute of Technology Rourkela, Government of India

Abstract: Water shows a very different trend while melting. Estimating the transition point of any material is still problematic. In recent time, several techniques have been involved to simplify things. Due to anomalous behaviors of water, it's transition properties are different from conventional substances. This study is an approach to understand the mechanism of phase transition using computer simulation. For better understanding the mechanism, it is vital to have knowledge of interatomic interaction of the water system. There are several potential models available for water like SPC/E, TIP3P, TIP4P etc. Another potential model, Stillinger-Weber potential model is good enough to predict the properties of water. This model considers two and three particle interactions. That model of water is named as monoatomic water(mW). The Anomaly behaviors of water are well predicted using mW model of water. Difference in free energy connecting two phases of water is evaluated using reversible thermodynamic route. Supercritical path is established using more than one path. These thermodynamic paths are reversible. The best of my knowledge, this is first approach to apply thermodynamic path for a system where volume of solid state is more compare to volume of liquid during phase transformation. Transition point is determined Gibbs free energy. Abrupt change in the density as function of temperature is observed. Hysteresis loop is also observed for potential energy. For temperature higher than 285K, huge fall in density and potential are noticed, suggesting full transition from one phase to another.

Keywords: Molecular Dynamics, LAMMPS, Equations of state, Thermodynamic Path, Thermodynamic Integration

1. Introduction

Freezing and melting can be understood by the transition and first principles, even in thermodynamic equilibrium and negotiating through a radial symmetrical pair capacity for relatively simple systems. During phase transformation it shows anomalous behaviors compare to conventional elements and compounds. Exact mechanism of phase transformation of water becomes a challenging problem and remains unanswered[1-5].

Phase transition of water in confinement is reported[6]. Melting and freezing transition is reported based on Hansen-Verlet criteria[7]. The anomaly character of water is studied at low temperature[8]. Phase diagram is reported with influence of external force field[9]. Solidification of fluidic water is studied using TIP4P model[10-13]. Thermodynamic stability is reported for mW model[14].Transition temperature can also be evaluated using specific heat capacity information[15,16]. Another robust technique for determination of transition point is calculation of entropy[17, 18]. Conventional methods like density hysteresis plot, Lindemann parameter[5], non-Gaussian parameter[15], radial distribution function, structure factor, orientation order parameter etc are employed to predict the transition point of a material.

Solid to liquid transformation of Lennard-Jones(LJ) system under confinement is reported[16]. Transition point is determined on the basis of density hysteresis plot, Lindemann parameter, non-Gaussian parameter, radial distribution function, structure factor, orientation order parameter[16]. From sudden jump in density, one can determine the transition point. Similar kind of phenomena is also observed in potential energy. However, density changes observed after complete phase transformation. So determined transition point is not accurate. Other parameters are Lindemann parameter and non-Gaussian parameter. From the Lindemann parameter value one can estimate the melting and freezing transition point. For determination of melting transition, Change in first and second co-ordination number is important too[15].

Most of the above-mentioned methods are not accurate to predict the melting transition[17]. Estimated melting temperature is often higher compare to true melting temperature. Melting transition can be predicted more precisely using the knowledge of free energy. Transition temperature of Lennard-Jones(LJ) and sodium Chloride(NaCl) is reported from free energy information[18]. Free energy is evaluated employing thermodynamic integration. The thermodynamic route connecting solid-liquid is constructed employing reversible thermodynamic route[17, 18]. Phase transformation from solid to liquid under slit[19, 20] and cylindrical confinement is studied using free energy analyses[21]. Various melting and freezing criteria are reported using non-equilibrium method[22].

Gibbs free energy is the extensive property to analysis a system. Free energy gap between states is estimated deploying pseudo supercritical path[18]. This work is mainly focusing on evaluation of free energy barrier connecting solid-liquid during phase transitions. Melting temperature can be predicted using Gibbs free energy. Gibbs free energy calculation involves with thermodynamics integration and multiple histogram reweighting(MHR) method[18]. Estimation of true thermodynamic temperature is evaluated with the help of pseudo-supercritical reversible thermodynamic cycle along the help of equation of states. Thermodynamic path is established using more than one reversible thermodynamic path. Thermodynamic integration is performed using Gauss-Quadrature integration scheme.

In this work, I evaluate free energy gap connecting solid-liquid transitions. Due to very small density difference between two phases make the simulations more complicated. I present briefly the technique. (a) The liquid state is transformed into a poorly interacting liquid with the help of slowly decreasing the interatomic attractions. (b) Gaussian wells are located to the corresponding particles; simultaneously the volume is enlarged to obtain a poorly interacting oriented state. (c) Gaussian wells are removed gradually and simultaneously interatomic attractions are slowly brought back to its whole strength to obtain a crystalline state.

2. Methodology

In this work, I evaluate the free energy connecting solid-liquid state transition. The inclusive technique is described elsewhere [17]. However, I present very shortly the technique for the comprehensive understanding of the reader. The estimation of phase transition point from free energy analysis is combination of four stages. First step is evaluation of an approximate transition point from quenching and heating method. Second is estimation of free energy for the solid state with respect solid reference state. Similarly for liquid phase is also determined with respect to liquid reference state. Equation of states are generated using multiple histogram reweighting technique[21]. Third stage is the computation of gap in free energy connecting two states at an estimated transition point[21]. Free energy computation is performed with the help of pseudo-supercritical transformation path. Then ultimately with the help of second and third steps evaluation of the transition point is done at zero energy difference[21]. That point is considered as true thermodynamic transition point. Each step is exclusively elaborated

below. Interaction potential of water(mW) is as follows:

$$E = U_{inter}(r^N) = \sum_i \sum_{j>i} \varphi_2(r_{ij}) + \sum_i \sum_{j\neq i} \sum_{k>j} \varphi_3(r_{ij}, r_{ik}, \theta_{ijk}) \quad (1)$$

$$\varphi_2(r_{ij}) = A_{ij}\epsilon_{ij}\left[B_{ij}\left(\frac{\sigma_{ij}}{r_{ij}}\right)^{p_{ij}} - \left(\frac{\sigma_{ij}}{r_{ij}}\right)^{q_{ij}}\right] exp\left(\frac{\sigma_{ij}}{r_{ij}-a_{ij}\sigma_{ij}}\right) \quad (2)$$

$$\varphi_3(r_{ij}, r_{ik}, \theta_{ijk}) = \lambda_{ijk}\epsilon_{ijk}\left[cos\theta_{ijk} - cos\theta_{0ijk}\right]^2 exp\left(\frac{\gamma_{ij}\sigma_{ij}}{r_{ij}-a_{ij}\sigma_{ij}}\right) exp\left(\frac{\gamma_{ik}\sigma_{ik}}{r_{ik}-a_{ik}\sigma_{ik}}\right) \quad (3)$$

The φ_2 represents two particles interaction term. The φ_3 presents three particles attraction expression. The summation in the expression are overall neighbors J and K of atom I within a truncated length a[23]. The A, B, p, and q parameters employed for two-particles attractions. The λ and $\cos\theta_0$ parameters are used only for three-particles attractions. The ϵ, σ and a parameters employed for both cases. γ is employed for three-particles attraction. However, this is classified for pairs of atoms. The others extra parameters are dimensionless[23].

Table 1: Value of parameters used in mW potential(in real unit)

A	B	P	Q	A	λ	γ	ε(kcal)	σ(Å)
7.0495562	0.6022245	4	0	1.80	23.15	1.20	6.189	2.3925

2.1 Estimation of an estimated transition temperature

To detect an approximate transition temperature, gradually heating and quenching simulations are performed for solid and liquid states, respectively[21], by employing *NPT* simulation at P = 1.0 bar. Around 36864 number of particles are used in simulation. Afterwards, the estimated transition temperature is chosen within the metastable region at where a sudden change in the density is noticed[21].

2.2 Solid and liquid free energy curve with respect to their corresponding reference states

The next stage is the formation of the Gibbs energy. The Gibbs energy is expressed in terms of temperature. They are presented for both states with regard to their corresponding standard phase temperature. This free energy curves are obtained over a small region around the estimated transition point at the constant pressure[21]. The temperature range is given in Eq. 16. Using the free energy connecting the two states at the estimated transition point., the pure state corresponding free energy plots are altered to the solid-liquid free energy difference in the terms of temperature, which is required to determine the transition point where the gap in energy connecting solid and liquid states is zero[21]. This is carried out using multiple histogram reweighting(MHR) technique. Multiple histogram reweighting(MHR) diagrams are formed the from knowledge of volume and potential energy of the system.

2.3 Computation of solid-liquid free energy gap at an estimated transition point

The Helmholtz free energy gap connecting the solid and liquid states at an estimated transition point is estimated by forming a reversible way connecting the solid and liquid states with the help others reversible stages[21]. The free energy throughout the connecting route is evaluated using a known integration scheme:

$$\Delta A^{ex} = \int \langle \frac{dU}{d\lambda} \rangle_{NVT\lambda} \, d\lambda \quad (4)$$

while ΔA^{ex} is the gap in Helmholtz free energy. Kirkwood's coupling parameter is used by the symbol λ. Generally, λ changes in between 0 to 1. The value of $\lambda = 0$ system act as an ideal state[18]. The angled bracket is indication of ensemble average for a specific λ parameter[18]. The three stages pseudo-supercritical conversion method is represented in Fig. 1. Very short explanation of the stages is presented below.

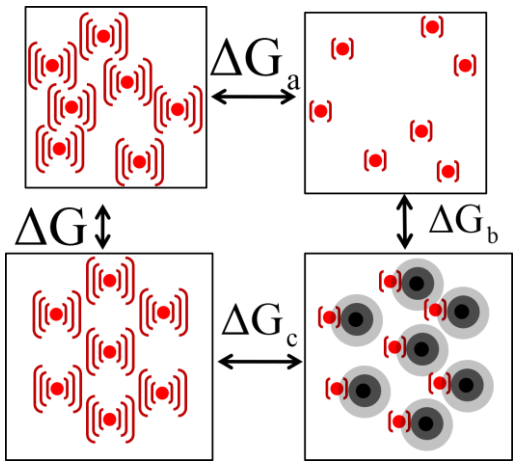

Figure : 1 presents the three stages pseudo-supercritical conversion route. (a) The liquid state is transformed into a poorly interacting liquid by slowly increasing the coupling parameter[18]. *(b) Gaussian wells are located to the corresponding particles; simultaneously the volume is enlarged to obtain a poorly interacting oriented state. (c) Gaussian wells are removed gradually while coupling parameter is slowly increasing to bring back its full strength to obtain a crystalline state.*

1. Stage-a

Initially, strongly attracted liquid state is transformed into a poorly interacting liquid using a coupling parameter λ, which controls interatomic potential[18] in the mentioned way:

$$U_a(\lambda) = [1 - \lambda(1 - \eta)]U_{inter}(r^N) \quad (5)$$

where $U_{inter}(\mathbf{r}^N)$ is the interatomic interaction energy due to location of all N particles[18]. The η is a scaling parameter. The value varies $0 < \eta < 1$. The first derivative of intermolecular interaction relation produces:

$$\frac{\partial U_a}{\partial \lambda} = -(1 - \eta)U_{inter}(r^N) \quad (6)$$

2. Stage-b

During second stage, volume of liquid state is enlarged to the volume of solid state unlike other conventional substances. Enlarge volume is clearly visible in Fig. 1. This stage is most complicated among the three stages. The minute densities difference between two phases becomes challenging in this stage. Hence, length of the simulation box (L_x, L_y *and* L_z) for a particular system dimension must be predetermined at the estimated transition point, either from the MHR results or hysteresis diagram[18]. Liquid box dimension is 10.318570 nm(H_l) and solid phase dimension is 10.401820 nm(H_s). Greater solid phase dimension compare to liquid phase dimension make the simulation more complicated. The change in simulations' box dimension confirms that pressures remain unaltered at the start of thermodynamic path and at the completion of stage-c, which is presented in Fig. 7. The interatomic interaction on the basis of λ in this stage is represented following way:

$$U_b(\lambda) = \eta U_{inter}[r^N(\lambda)] + \lambda U_{Gauss}[r^N(\lambda), r^N_{well}(\lambda)] \quad (7)$$

where $\mathbf{r}^N(\lambda)$ and $\mathbf{r}_{well}{}^N(\lambda)$ are the representation of the positions of atoms and Gaussian wells respectively[18]. These coordinates are purely function of *coupling parameter* due to the change in simulation dimension. U_{Gauss} presents interatomic potential because of the attraction in between the wells and corresponding particles(Eq.9). The values of parameters 'a' and 'b' are taken from Gochola's works[17]. Particles coordinates due to enlarge volume from liquid to solid conversion follow the same manner as did in literature[18]. $H(\lambda)$ denotes box dimension at any value of coupling parameter λ. Equation 8 represents change in box dimension for coupling parameter values.

$$H(\lambda) = (1 - \lambda)H_l + \lambda H_s \quad (8)$$

$$U_{Gauss}[r^N(\lambda), r^N_{well}(\lambda)] = \sum_{i=1}^{N}\sum_{k=1}^{N_{wells}} a_{ik} exp[-b_{ik} r^2_{ik}(\lambda)] \quad (9)$$

$$-\frac{\delta U_{inter}}{\delta H_{xz}} = \sum_y P^{ex}_{xy} V H^{-1}_{zy} \quad (10)$$

Derived form of potential expression with respect to λ is

$$\frac{\partial U_b}{\partial \lambda} = -\sum_{x,y,z} V(\lambda) H^{-1}_{zy}(\lambda) \Delta H_{xz} \left(\eta P^{ex}_{xy} + \lambda P^{ex}_{Gauss,xy}\right) + U_{Gauss}[r^N(\lambda), r^N_{well}(\lambda)] \quad (11)$$

3. Stage-c

Stage-c is ultimate step of the pseudo-supercritical conversion method[18]. In this stage fully interacting solid configurationally phase is obtained. The interaction potential is presented of this final step in terms of λ

$$U_c(\lambda) = [\eta + (1 - \eta)\lambda]U_{inter}(r^N) + (1 - \lambda)U_{Gauss}[r^N(\lambda), r^N_{well}(\lambda)] \quad (12)$$

And the derivative terms can be rewritten:

$$\frac{\partial U_c}{\partial \lambda} = (1 - \eta)U_{inter}(r^N) + U_{Gauss}[r^N(\lambda), r^N_{well}(\lambda)] \quad (13)$$

2.4 Determination of transition point where ΔG is zero

The free energy ΔA^{ex}, between phases at the estimated transition point is evaluated by thermodynamic integration[18]. Now transfer of the Helmholtz energy into the Gibbs energy is important. It is obtained using the formulae given, $\Delta G = \Delta A^{ex} + \Delta A^{id} + P\Delta V$. The expression ΔA^{ex} is computed using reversible transformation path method. The second term ΔA^{id} is the contribution from ideality. Final term in the expression is work term due to change in volume from solid to liquid phase. Additionally, the histogram reweighting method produces two equations of states. Expression of the liquid state, $[(\beta G)_{T_1,l} - (\beta G)_{T_i,l}]$ is familiar and for the solid state expression is $[(\beta G)_{T_1,s} - (\beta G)_{T_i,s}]$[18], the term $(\beta G)_{Tm,n}$ expresses (βG) for hysteresis loop region at the estimated temperature T_{em}[21], provided that T_{em} is estimated transition temperature, is the transition temperature st which the reversible thermodynamic path[21] is performed[18], achieved the following:

$$[(\beta G)_{T_1,l} - (\beta G)_{T_{em},s}] + [\beta(G_{T_{em},s} - G_{T_{em},l})] - [(\beta G)_{T_i,l} - (\beta G)_{T_{em},l}] = [(\beta G)_{T_1,s} - (\beta G)_{T_i,l}] \quad (14)$$

Eq. 10 further can be rearranged as:

$$[(\beta G)_{T_1,l} - (\beta G)_{T_{em},s}] + [\beta(G_{T_{em},s} - G_{T_{em},l})] + [(\beta G)_{T_1,l} - (\beta G)_{T_i,l}] - [(\beta G)_{T_1,l} - (\beta G)_{T_{em},l}] = [(\beta G)_{T_1,s} - (\beta G)_{T_i,l}] \quad (15)$$

Where, all the terms except second term of Eq.11 is achieved using the multiple histograms reweighting method, Whereas; the second term is determined using three stages reversible thermodynamic path using thermodynamic integration.

3. Simulation Details and Software Work

3.1 Molecular Dynamics Simulation:

Molecular dynamics simulation is a technique used to get insights about the movements and properties of a system of atoms and molecules. It is basically a computer simulation where the system of atoms and molecules are given to make interaction among themselves for a certain amount of period. As a result, we can predict the outcome of various real-world systems by computer simulations without the need for experiments. MD helps to do it in different length and time scales. It is said to bridge the gap between theory and experiments. Various parameters involving in a system's interaction is calculated in molecular dynamics simulation.

3.2 Atomic Potential Used

Stillinger-Weber Potential is a good model for mW water. It considers both two-particle and three-particle interactions. The values of following parameters in metal units have been used. The potential of the water is provided in Eq. 1, 2 and 3. Parameters values are listed in Table. 1.

3.3 Simulation Details and Potential Model

The NPT MD simulations are conducted with the help of LAMMPS[23]. Unit system of the simulation process is metal. The integration of equation is performed employing velocity-Verlet algorithm. Integration time step (Δt) is 5 fs. The temperature is monitored using a Nose´–Hoover thermostat. The pressure is monitored using Nose´–Hoover barostat. The time relaxation is of 1ps. The pressure relaxation is of 5ps. Number of particles are simulated around 36684. The periodic boundary condition is applied for simulations. During quenching, the initial liquid configurations are taken as ideal diamond structures at 350k. Cooling process is carried out gradually after each 5000,000 MD time steps. Change of temperature T is 2k for each NPT simulation. Total run time around 50ns. The rate of heating or cooling is 2K/50ns. Temperature is dropped from 350k to 150k with a decrement of 2K. At the

time of heating process, the last configuration of the quenching simulation is initial co-ordinate of the heating system. Heating is also conducted same way as the quenching. The increment of temperature T is 2K for each NPT simulation. Process of heat supply is done until the solid has completely converted into liquid. Temperature range of heating is from 150k to 350k. The density is determined at every interval of temperature from the knowledge of simulation volume, number of particles and molecular weight of the water. The Gibbs energy gap for connecting states is estimated at transition temperature using pseudo-super-critical path. The true transition point is estimated at a point, Gibbs free energy gap connecting two states reach zero. Initially, I select an estimated transition point, T_{em}. The two different types of *NPT* simulations are carried out by LAMMPS[25]. The velocity-verlet algorithm is employed throughout all simulations. Integration time step is Δt= 5 fs. The temperature is monitored using a Nose´–Hoover thermostat. The pressure is monitored using Nose´–Hoover barostat. The time relaxation is of 1ps for temperature. The pressure relaxation is of 5ps. 36864 Number of particles are used. Throughout the simulations process, applied boundary conditions for in all the three dimensions are periodic. The constructions of equations of states for both phases are done employing multiple histogram reweighting diagrams. Histograms are generated from *NPT* simulations based on volume and potential energy of the system. Total 17 simulations are carried out for individual phase. The temperature is selected in accordance with the given formulae

$$T_i = T_{em} + \sum_{n=-9}^{9} n\Delta T \quad (16)$$

Where T_{em} is the expected transition point computed from the density vs. temperature plot hysteresis data; $\Delta T(=5\,°K)$ is determined based on size of the with meta-stable region.

The initial configurations for both phases are used from previous simulation run. The sufficient equilibration, run is performed duration of around 200 ps. The total simulation run time is for 10ns. The standard reference temperatures are chosen at the minimum point, $T_i = T_{em} - 9\Delta T$. Histograms are generated base potential energy and volume of system.

For the reversible path evaluation (for the three steps of pseudo-supercritical path)as shown in figure 1, simulations are carried with *NVT* ensemble. The Nose´-Hoover thermostat algorithm is employed for temperature and pressure. The value of Gaussian parameters are selected in accordance with Grochola[17]. The scaling parameter is constant at η = 0.1[18].

Simulations of Stage-a of the reversible thermodynamic path are initialized from a random initial co-ordinates of the particles. These co-ordinates are achieved during heating quenching simulations. After that for every coupling parameter value initial configuration is obtained from simulation[18]. Total run time for each simulation of three stages for each λ value is 60ns, time step of integration is 10fs. Total run time for each coupling parameter value is 60 ns[21]. During the stage-b of three stages, final co-ordinates of step-1 are the starting point. But, to achieve the Gaussian potential wells another 36864 atoms are situated on its corresponding lattice point[18]. Now for final stage last configuration of stage-b for the third stage is taken as initial configuration. The way the three stages are performed the pressures of the system remains constant before and after of the transformation path as shown in figure 7. Integration for three stages are performed with ten, fifteen and twenty points Gauss-Legendre integration techniques[18].

4. Results and Discussions

In this portion I try to describe output results of various parameters like density, potential energy and free energy with the change in temperature and coupling parameter(λ). Based on the variation of these parameters, I will try to formulate a basic idea about the melting of water system.

4.1 Density

In this part I describe the nature of density of the water system as I perform heating and quenching. Sharp density changed is observed for both the heat and quenching case. During cooling the system as shown in figure 2 I obtain maximum density 1.003362 gm/cc at temperature 250K and minimum density 0.977756gm/cc at temperature 202K. Results is well agreement with literature value[24]. Quenching and heating path are not reversible as shown in figure 3, for this reason hysteresis loop is formed. That indicates first order phase transition. It can be observed that in the heating process, there is a sudden increase in the density of the system around 225K. Also, in the quenching process sudden decrease in the density can be seen around 200K. The plot clearly forms a hysteresis. This is an indication of first order phase change. Density plot shows anomaly behavior towards the phase transition. Metastable region is observed in middle portion of the hysteresis curve. True melting temperature lies in this loop. Vertical line indicates an approximate estimated transition point; corresponding horizontal lines indicate density of liquid and solid phase. These densities determine the solid phase(L_x=10.401820 nm) and liquid phase(L_x=10.318570 nm) box dimension for the reversible thermodynamic route.

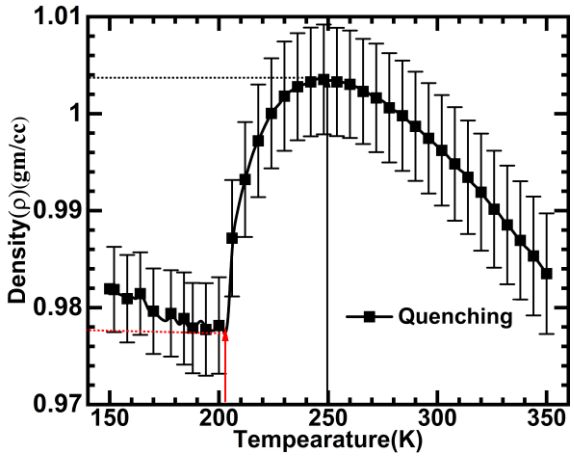

Figure 2: *figure represents density as function of temperature. The vertical upward arrow black in color indicates maximum density(1.003362gm/cc) temperature(TMD=250K) and the vertical upward arrow red in color indicates minimum density(0.977756gm/cc) temperature(TmD=202K). Horizontal dotted lines black and red in color indicate corresponding density for TMD and TmD respectively.*

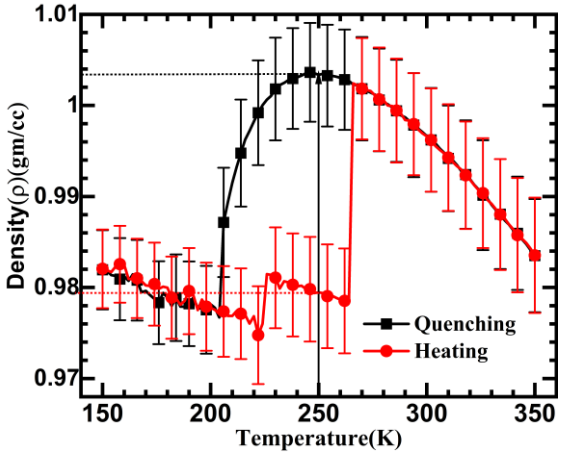

Figure 3: figure represents density vs. temperature plot. Filled square black in color represents the quenching system whereas filled circle for heating the system. Quenching and heating curves do not follow the same path which indicates first order transition. Hysteresis loop is clearly observed in density temperature plot. Metastable region is noticed middle of the curve and true transition point lies in this meta-stable region. Vertical arrow line indicates an estimated estimate transition point(T_{em} = 250K) .Horizontal black line and red line indicate corresponding liquid density(1.003362) and solid density(0.979466) respectively at estimated melting temperature. From where one can determine liquid phase as well as solid phase box dimension

Potential energy also shows the similar kind of behavior like density which is shown in figure 4 below. The red rectangle represents heating process. The black circle represents quenching process.

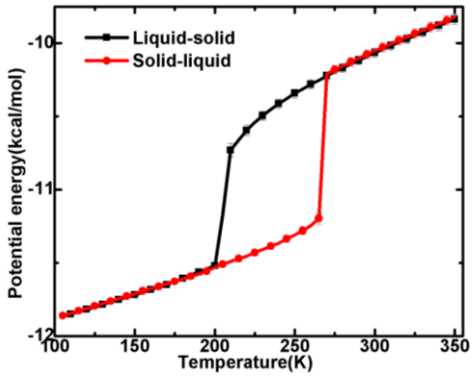

Figure:4 potential energy in terms of temperature similar kind of nature is obtained as density vs. temperature curve. Filled square black in color represents cooling process whereas red circle represents heating process.

4.2 Free energy

Helmholtz free energy difference between liquid-and solid phase is determined using pseudo-supercritical path by constructing reversible thermodynamic paths [17]. Thermodynamics integration is performed using Gauss-quadrature integration scheme. At the beginning of the reversible path the interaction potential is changing according to Eq. 5. Integration is carried out using 10, 15 and 20 points. No significance difference is observed due to different data points. Derivative of interaction potential energy with respect to λ presents in Fig. 5 below. For the λ values they coincide as shown in figure 5. Figure 7 and 8 represent for stage-b and stage-c respectively. The whole thermodynamic path is performed such a way that pressure remain unchanged at beginning and at the end of the path, as shown in figure 6. During stage-b interaction potential and box dimensions are changing in accordance with Eq.7 and 8 respectively. Simultaneously Gaussian potential wells are interacting between particles and its corresponding lattice points as per Eq. 9. In the conclusion of the pseudo-super-critical route the interaction potential follows the Eq.11. The derivative of potential energy with respect to coupling parameter in stage-b is represented in Fig. 7. The path is reversible and smooth. Similarly the derivative of potential energy with respect to coupling parameter in stage-c is represented in Fig. 8. Figures for all the stages are smooth and reversible, so we can easily integrate it. The Gibbs free energy difference connecting solid-liquid is around 0.101025±0.00135kcal/mol. Results are reported in Table 2 below. Equation of state or the Gibb free energy for both liquid and solid phases with respect to their respective reference state is determined using multiple histogram diagrams(MHR). Histograms are developed by collecting potential energy and volume of the system. Using the Gibbs free energy difference between solid-liquid obtained from pseudo-supercritical path, along with equation of state which is obtained from multiple histogram reweighting(MHR) method, the equation of states are converted into single reference state using Eqn. 14 and 15. The gap in free energy connecting two phases are determined and presented in Fig. 9. True thermodynamic melting temperature is the point where ΔG is zero. From Fig. 9 it is clear that true thermodynamic transition point is around 273.9±0.9°K.

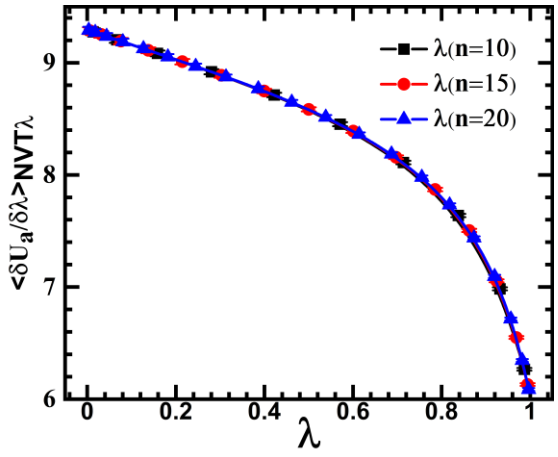

Figure: 5 $\langle \partial U_a / \partial \lambda \rangle_{NVT\lambda}$ *as a variable of* λ *for three* λ *types values(10,15 and 20) of Stage-a for pseudo supercritical path . Thermodynamic path is smooth and reversible, hence integrable. Error is so small it submerges with symbol. There is no significant difference among them for stage-a of pseudo-supercritical transformation path*

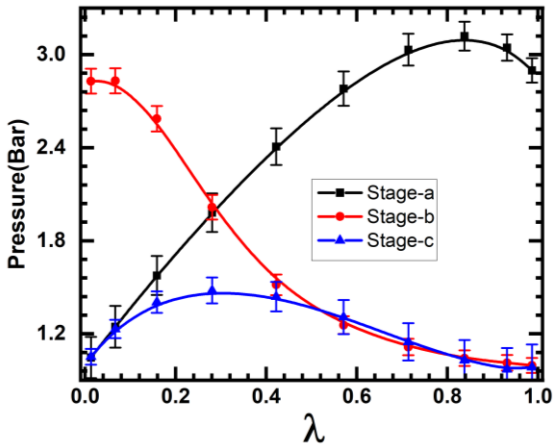

Figure : 6 Pressure at the start of stage-a and at the end of stage-c is constant. This is essential and the sufficient criteria for construction of the thermodynamic reversible paths.

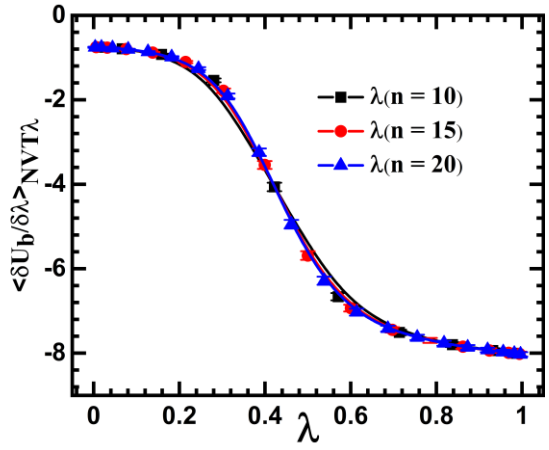

Figure : 7 $\langle \partial U_b / \partial \lambda \rangle_{NVT\lambda}$ *as a variable of* λ *(10,15and 20) of Stage-b values. Thermodynamic path is smooth and reversible, hence integrable. Error is so small it submerges with symbol.*

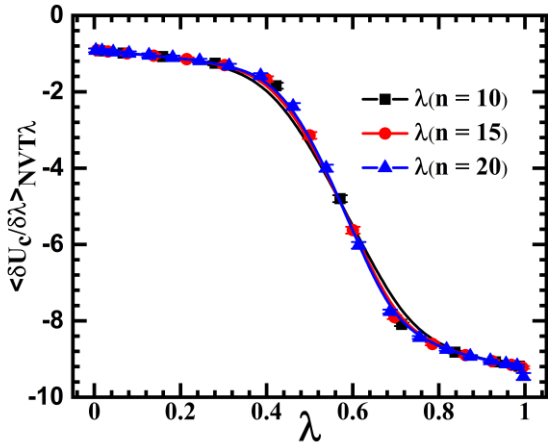

Figure : *8* $\langle \partial U_c / \partial \lambda \rangle_{NVT\lambda}$ *as a variable of* λ*(10,15 and 20) for stage-c. Thermodynamic path is smooth and reversible, hence integrable.*

Table: 2. Separation of the subscriptions to the gap in Gibbs free energy connecting the two states *T*= 250°K .The pressure is maintained at *P= 1 Bar* for the water system(mw model,Stillinger-Weber Potential).

Free Energy Terms(kcal/mol)	
$A_s^{*ex} - A_l^{*ex}$	11.989193±0.00135
$A_s^{*\iota\omega} - A_l^{*\iota\omega}$	-11.931945
$P^*\Delta V^*$	0.043769
$G_s^* - G_l^*$	0.101025±0.00135

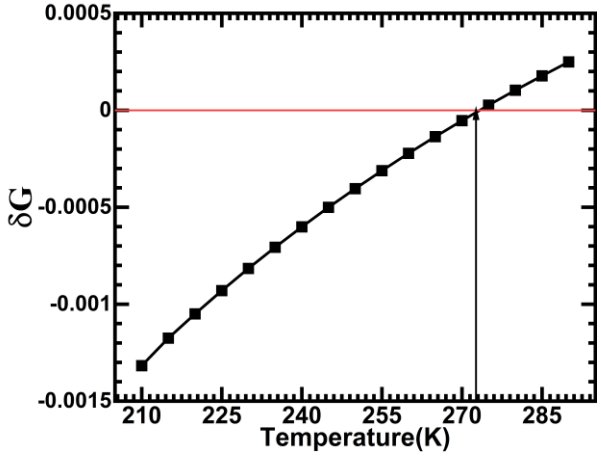

Figure : 9 ΔG as a function of T. Vertical arrow line blue in colour indicates solid-liquid transition point temperature or true thermodynamic transition temperature temperature(T_m) of solid where Gibbs free energy difference, ΔG, between soli d and liquid is zero.

5. Conclusion

Various methods have been employed and I have been successful in observing the phase transformation of water, depending on various parameters. While simulating with decreasing temperature, this is the value for density after the melting occurred at approximately 273.9±0.9° K, which is slightly higher than the reported melting point for water which is 273.15 K.

Also, keeping in mind the long-established meaning of solid to liquid phase transition, the jump in potential energy is also used to indicate the melting stage of any substance. Anomaly behavior is observed in density of water system, which makes it more complicated to implement pseudo-supercritical thermodynamic path.

Phase transition point is determined basing on Gibbs free energy. Estimation of Gibbs free energy is performed with the help of pseudo-supercritical reversible thermodynamic cycle along with the help of multiple histogram reweighting diagrams. The construction of supercritical path is the combination of three stages. The thermodynamic integration is applied using 10, 15 and 20 points. The thermodynamics integration is insignificant in respect of the number of data points, which are shown in all stages. Estimated true thermodynamics melting temperature is around 273.9°K± 0.9°k, which is in good precision with experimental results. Accuracy of determined melting temperature from free energy analysis is better than any other methods.

I have been successful in implementing pseudo-supercritical route to evaluate gap in free energy connecting the two phases for complicated interaction potential model. I performed the simulations with significantly large number of particles. In future one can study the confinement effect on anomalous phase transition of water using free energy analysis.

6. References

1. R.W.Cahn, *Melting from within.* Nature, 2001. **413**: p. 582-583.
2. H,S.F., *A Topographic View of Supercooled Liquids and Glass Formation.* Science,1995.**267**(5206): p. 1935-1939.
3. Stillinger, F.H. and T.A. Weber, *Computer simulation of local order in condensed phases of silicon.* Phys. Rev. B, 1985. **31**(8): p. 5262-5271.
4. Stillinger, F.H. and T.A. Weber, *Point defects in bcc crystals: Structures, transition kinetics, and melting implications.* J. Chem. Phys., 1984. **81**(11): p. 5095-5102.
5. Stillinger, F.H. and T.A. Weber, *Lindemann melting criterion and the Gaussian core model.* Phys. Rev. B, 1980. 22(8): p. 3790-3794.
6. Moore, E.B., et al., *Freezing, melting and structure of ice in a hydrophilic nanopore.* Phys. Chem. Chem. Phys., 2010. **12**: p. 4124–4134.
7. Hansen, J.-P. and L. Verlet, *Phase Transitions of the Lennard-Jones System.* Phy. Rev., 1969. **184**(1): p. 151-161.
8. Stanley, H.E., et al., *The puzzling behavior of water at very low temperature Invited Lecture.* Phys. Chem. Chem. Phys., 2000. **2**: p. 1551 - 1558.
9. James, T. and D.J. Wales, *Energy landscapes for water clusters in a uniform electric field.* J. Chem. Phycs., 2007. **126**: p. 054506-1 - 054506-12.
10. Moore, E.B. and V. Molinero, *Ice crystallization in water's "no-man's land".* J. Chem. Phys., 2010. **132**(24): p. 244504-1 - 244505-10
11. Moore, E.B. and V. Molinero, *Structural transformation in supercooled water controls the crystallization rate of ice.* Nature, 2011. **479**: p. 506-509.
12. Moore, E.B. and V. Molinero, *Is it cubic? Ice crystallization from deeply supercooled water.* Phys. Chem. Chem. Phys., 2011. **13**: p. 20008–20016.
13. Moore, E.B., et al., *Freezing, melting and structure of ice in a hydrophilic nanopore.* Phys. Chem. Chem. Phys., 2010. **12**: p. 4124–4134.
14. Jacobson, L.C., W. Hujo, and V. Molinero, *Thermodynamic Stability and Growth of Guest-Free Clathrate Hydrates: A Low-Density Crystal Phase of Water.* J. Phys. Chem. B 2009, 113, , 2009. **113**: p. 10298–10307

15. Zhang, S.L., et al., The study of melting stage of bulk silicon using molecular dynamics simulation. Physica B, 2011. **406**: p. 2637-2641.
16. Das, C.K. and J.K. Singh, Melting transition of confined Lennard-Jones solids in slit pores. Theor. Chem. Acc, 2013. **132**: p. 1351.
17. Grochola, G., Constrained fluid λ-integration: Constructing a reversible thermodynamic path between the solid and liquid state. J. Chem. Phys., 2004. **120**: p. 2122.
18. Eike, D.M., J.F. Brennecke, and E.J. Maginn, Toward a robust and general molecular simulation method for computing solid-liquid coexistence. J. Chem. Phys., 2005. **122**: p. 014115.
19. Das, C.K. and j.K. Singh, Effect of confinement on the solid-liquid coexistence of Lennard-Jones Fluid. J. Chem. Phys., 2013. **139**(17): p. 174706.
20. Das, C.K. and J.K. Singh, Melting transition of confined Lennard-Jones solids in slit pores. Theor Chem Acc, 2013. **132(4)**: p. 1351-1 – 1351-13.
21. Das, C.K. and J.K. Singh, Melting transition of Lennard-Jones fluid in cylindrical pores. J. Chem. Phys., 2014. **140**(20): p. 204703-1 - 204703-9.
22. Hoffmann, G.P. and H. L¨owen, Freezing and melting criteria in non-equilibrium. J. Phys.: Condens. Matter, 2001. **13**: p. 9197-9206.
23. J, P.S., Fast Parallel Algorithms for Short–Range Molecular Dynamics. J. Comp. Phys., 1995. **117**: p. 1-9.
24. Moore, E.B. and V. Molinero, Growing correlation length in supercooled water. J.Chem.Phys**.** , 2009. **130**(24): p. 2445505-1-2445505-12.